

A Measurement of Charged Particle Multiplicity in $Z^0 \rightarrow c\bar{c}$ and $Z^0 \rightarrow b\bar{b}$ Events

The OPAL Collaboration

Abstract

We have used data from the OPAL detector at LEP to reconstruct D^* mesons and secondary vertices in jets. We have studied the hemispheres of the events opposite these jets and obtain values of the hemisphere charged particle multiplicity in $Z^0 \rightarrow u\bar{u}, d\bar{d}, s\bar{s}, Z^0 \rightarrow c\bar{c}$ and $Z^0 \rightarrow b\bar{b}$ events of

$$\begin{aligned}\bar{n}_{uds} &= 10.41 \pm 0.06 \pm 0.09 \pm 0.19 \\ \bar{n}_c &= 10.76 \pm 0.20 \pm 0.14 \pm 0.19 \\ \bar{n}_b &= 11.81 \pm 0.01 \pm 0.12 \pm 0.21\end{aligned}$$

where the first errors are statistical, the second systematic and the third a common scale uncertainty. We find the difference in total charged particle multiplicity between c and b quark events and light (u, d, s) quark events to be

$$\begin{aligned}\delta_{cl} &= 0.69 \pm 0.51 \pm 0.35 \\ \delta_{bl} &= 2.79 \pm 0.12 \pm 0.27.\end{aligned}$$

These results are compared to the predictions of various models and QCD based calculations.

(Submitted to Physics Letters)

The OPAL Collaboration

R. Akers¹⁶, G. Alexander²³, J. Allison¹⁶, K. Ametewee²⁵, K.J. Anderson⁹, S. Arcelli², S. Asai²⁴,
D. Axen²⁹, G. Azuelos^{18,a}, A.H. Ball¹⁷, E. Barberio²⁶, R.J. Barlow¹⁶, R. Bartoldus³,
J.R. Batley⁵, G. Beaudoin¹⁸, A. Beck²³, G.A. Beck¹³, C. Beeston¹⁶, T. Behnke²⁷, K.W. Bell²⁰,
G. Bella²³, S. Bentvelsen⁸, P. Berlich¹⁰, S. Bethke¹⁴, O. Biebel¹⁴, I.J. Bloodworth¹, P. Bock¹¹,
H.M. Bosch¹¹, M. Boutemeur¹⁸, S. Braibant¹², P. Bright-Thomas²⁵, R.M. Brown²⁰, A. Buijs⁸,
H.J. Burckhart⁸, R. Bürgin¹⁰, C. Burgard²⁷, N. Capdevielle¹⁸, P. Capiluppi², R.K. Carnegie⁶,
A.A. Carter¹³, J.R. Carter⁵, C.Y. Chang¹⁷, C. Charlesworth⁶, D.G. Charlton^{1,b}, S.L. Chu⁴,
P.E.L. Clarke¹⁵, J.C. Clayton¹, S.G. Clowes¹⁶, I. Cohen²³, J.E. Conboy¹⁵, O.C. Cooke¹⁶,
M. Cuffiani², S. Dado²², C. Dallapiccola¹⁷, G.M. Dallavalle², C. Darling³¹, S. De Jong¹²,
L.A. del Pozo⁸, H. Deng¹⁷, M. Dittmar⁴, M.S. Dixit⁷, E. do Couto e Silva¹², J.E. Duboscq⁸,
E. Duchovni²⁶, G. Duckeck⁸, I.P. Duerdoth¹⁶, U.C. Dunwoody⁵, J.E.G. Edwards¹⁶,
P.A. Elcombe⁵, P.G. Estabrooks⁶, E. Etzion²³, H.G. Evans⁹, F. Fabbri², B. Fabbro²¹, M. Fanti²,
P. Fath¹¹, M. Fierro², M. Fincke-Keeler²⁸, H.M. Fischer³, P. Fischer³, R. Folman²⁶, D.G. Fong¹⁷,
M. Foucher¹⁷, H. Fukui²⁴, A. Fürtjes⁸, P. Gagnon⁶, A. Gaidot²¹, J.W. Gary⁴, J. Gascon¹⁸,
N.I. Geddes²⁰, C. Geich-Gimbel³, S.W. Gensler⁹, F.X. Gentit²¹, T. Gerasis²⁰, G. Giacomelli²,
P. Giacomelli⁴, R. Giacomelli², V. Gibson⁵, W.R. Gibson¹³, J.D. Gillies²⁰, J. Goldberg²²,
D.M. Gingrich^{30,a}, M.J. Goodrick⁵, W. Gorn⁴, C. Grandi², E. Gross²⁶, J. Hagemann²⁷,
G.G. Hanson¹², M. Hansroul⁸, C.K. Hargrove⁷, P.A. Hart⁹, M. Hauschild⁸, C.M. Hawkes⁸,
E. Heflin⁴, R.J. Hemingway⁶, G. Herten¹⁰, R.D. Heuer⁸, J.C. Hill⁵, S.J. Hillier⁸, T. Hilse¹⁰,
P.R. Hobson²⁵, D. Hochman²⁶, R.J. Homer¹, A.K. Honma^{28,a}, R. Howard²⁹,
R.E. Hughes-Jones¹⁶, P. Igo-Kemenes¹¹, D.C. Imrie²⁵, A. Jawahery¹⁷, P.W. Jeffreys²⁰,
H. Jeremie¹⁸, M. Jimack¹, M. Jones⁶, R.W.L. Jones⁸, P. Jovanovic¹, C. Jui⁴, D. Karlen⁶,
J. Kanzaki²⁴, K. Kawagoe²⁴, T. Kawamoto²⁴, R.K. Keeler²⁸, R.G. Kellogg¹⁷, B.W. Kennedy²⁰,
B. King⁸, J. King¹³, J. Kirk²⁹, S. Kluth⁵, T. Kobayashi²⁴, M. Kobel¹⁰, D.S. Koetke⁶,
T.P. Kokott³, S. Komamiya²⁴, R. Kowalewski⁸, T. Kress¹¹, P. Krieger⁶, J. von Krogh¹¹,
P. Kyberd¹³, G.D. Lafferty¹⁶, H. Lefoux⁸, R. Lahmann¹⁷, W.P. Lai¹⁹, J. Lauber⁸, J.G. Layter⁴,
P. Leblanc¹⁸, A.M. Lee³¹, E. Lefebvre¹⁸, D. Lellouch²⁶, C. Leroy¹⁸, J. Letts², L. Levinson²⁶,
S.L. Lloyd¹³, F.K. Loebinger¹⁶, G.D. Long¹⁷, B. Lorazo¹⁸, M.J. Losty⁷, X.C. Lou⁸, J. Ludwig¹⁰,
A. Luig¹⁰, M. Mannelli⁸, S. Marcellini², C. Markus³, A.J. Martin¹³, J.P. Martin¹⁸,
T. Mashimo²⁴, W. Matthews²⁵, P. Mättig³, U. Maur³, J. McKenna²⁹, T.J. McMahon¹,
A.I. McNab¹³, F. Meijers⁸, F.S. Merritt⁹, H. Mes⁷, A. Michelini⁸, R.P. Middleton²⁰,
G. Mikenberg²⁶, D.J. Miller¹⁵, R. Mir²⁶, W. Mohr¹⁰, A. Montanari², T. Mori²⁴, M. Morii²⁴,
U. Müller³, B. Nellen³, B. Nijjhar¹⁶, S.W. O'Neale¹, F.G. Oakham⁷, F. Odorici², H.O. Ogren¹²,
N.J. Oldershaw¹⁶, C.J. Oram^{28,a}, M.J. Oreglia⁹, S. Orito²⁴, F. Palmonari², J.P. Pansart²¹,
G.N. Patrick²⁰, M.J. Pearce¹, P.D. Phillips¹⁶, J.E. Pilcher⁹, J. Pinfold³⁰, D.E. Plane⁸,
P. Poffenberger²⁸, B. Poli², A. Posthaus³, T.W. Pritchard¹³, H. Przysiezniak³⁰,
M.W. Redmond⁸, D.L. Rees⁸, D. Rigby¹, M.G. Rison⁵, S.A. Robins¹³, D. Robinson⁵,
N. Rodning³⁰, J.M. Roney²⁸, E. Ros⁸, A.M. Rossi², M. Rosvick²⁸, P. Routenburg³⁰, Y. Rozen⁸,
K. Runge¹⁰, O. Runolfsson⁸, D.R. Rust¹², M. Sasaki²⁴, C. Sbarra², A.D. Schaile⁸, O. Schaile¹⁰,
F. Scharf³, P. Scharff-Hansen⁸, P. Schenk⁴, B. Schmitt³, M. Schröder⁸, H.C. Schultz-Coulon¹⁰,
P. Schütz³, M. Schulz⁸, C. Schwick²⁷, J. Schwiening³, W.G. Scott²⁰, M. Settles¹², T.G. Shears⁵,
B.C. Shen⁴, C.H. Shepherd-Themistocleous⁷, P. Sherwood¹⁵, G.P. Siroli², A. Skillman¹⁵,
A. Skuja¹⁷, A.M. Smith⁸, T.J. Smith²⁸, G.A. Snow¹⁷, R. Sobie²⁸, S. Söldner-Rembold¹⁰,

R.W. Springer³⁰, M. Sproston²⁰, A. Stahl³, M. Starks¹², C. Stegmann¹⁰, K. Stephens¹⁶,
J. Steuerer²⁸, B. Stockhausen³, D. Strom¹⁹, P. Szymanski²⁰, R. Tafirout¹⁸, H. Takeda²⁴,
T. Takeshita²⁴, P. Taras¹⁸, S. Tarem²⁶, M. Tecchio⁹, P. Teixeira-Dias¹¹, N. Tesch³,
M.A. Thomson⁸, O. Tousignant¹⁸, S. Towers⁶, M. Tscheulin¹⁰, T. Tsukamoto²⁴, A.S. Turcot⁹,
M.F. Turner-Watson⁸, P. Utzat¹¹, R. Van Kooten¹², G. Vasseur²¹, P. Vikas¹⁸, M. Vincter²⁸,
A. Wagner²⁷, D.L. Wagner⁹, C.P. Ward⁵, D.R. Ward⁵, J.J. Ward¹⁵, P.M. Watkins¹,
A.T. Watson¹, N.K. Watson⁷, P. Weber⁶, P.S. Wells⁸, N. Wermes³, B. Wilkens¹⁰,
G.W. Wilson²⁷, J.A. Wilson¹, V-H. Winterer¹⁰, T. Wlodek²⁶, G. Wolf²⁶, S. Wotton¹¹,
T.R. Wyatt¹⁶, A. Yeaman¹³, G. Yekutieli²⁶, M. Yurko¹⁸, V. Zacek¹⁸, W. Zeuner⁸, G.T. Zorn¹⁷.

¹School of Physics and Space Research, University of Birmingham, Birmingham B15 2TT, UK

²Dipartimento di Fisica dell' Università di Bologna and INFN, I-40126 Bologna, Italy

³Physikalisches Institut, Universität Bonn, D-53115 Bonn, Germany

⁴Department of Physics, University of California, Riverside CA 92521, USA

⁵Cavendish Laboratory, Cambridge CB3 0HE, UK

⁶Carleton University, Department of Physics, Colonel By Drive, Ottawa, Ontario K1S 5B6, Canada

⁷Centre for Research in Particle Physics, Carleton University, Ottawa, Ontario K1S 5B6, Canada

⁸CERN, European Organisation for Particle Physics, CH-1211 Geneva 23, Switzerland

⁹Enrico Fermi Institute and Department of Physics, University of Chicago, Chicago IL 60637, USA

¹⁰Fakultät für Physik, Albert Ludwigs Universität, D-79104 Freiburg, Germany

¹¹Physikalisches Institut, Universität Heidelberg, D-69120 Heidelberg, Germany

¹²Indiana University, Department of Physics, Swain Hall West 117, Bloomington IN 47405, USA

¹³Queen Mary and Westfield College, University of London, London E1 4NS, UK

¹⁴Technische Hochschule Aachen, III Physikalisches Institut, Sommerfeldstrasse 26-28, D-52056 Aachen, Germany

¹⁵University College London, London WC1E 6BT, UK

¹⁶Department of Physics, Schuster Laboratory, The University, Manchester M13 9PL, UK

¹⁷Department of Physics, University of Maryland, College Park, MD 20742, USA

¹⁸Laboratoire de Physique Nucléaire, Université de Montréal, Montréal, Quebec H3C 3J7, Canada

¹⁹University of Oregon, Department of Physics, Eugene OR 97403, USA

²⁰Rutherford Appleton Laboratory, Chilton, Didcot, Oxfordshire OX11 0QX, UK

²¹CEA, DAPNIA/SPP, CE-Saclay, F-91191 Gif-sur-Yvette, France

²²Department of Physics, Technion-Israel Institute of Technology, Haifa 32000, Israel

²³Department of Physics and Astronomy, Tel Aviv University, Tel Aviv 69978, Israel

²⁴International Centre for Elementary Particle Physics and Department of Physics, University of Tokyo, Tokyo 113, and Kobe University, Kobe 657, Japan

²⁵Brunel University, Uxbridge, Middlesex UB8 3PH, UK

²⁶Particle Physics Department, Weizmann Institute of Science, Rehovot 76100, Israel

²⁷Universität Hamburg/DESY, II Institut für Experimental Physik, Notkestrasse 85, D-22607 Hamburg, Germany

²⁸University of Victoria, Department of Physics, P O Box 3055, Victoria BC V8W 3P6, Canada

²⁹University of British Columbia, Department of Physics, Vancouver BC V6T 1Z1, Canada

³⁰University of Alberta, Department of Physics, Edmonton AB T6G 2J1, Canada

³¹Duke University, Dept of Physics, Durham, NC 27708-0305, USA

^aAlso at TRIUMF, Vancouver, Canada V6T 2A3

^b Royal Society University Research Fellow

1 Introduction

The study of heavy quark production in Z^0 decays, where the centre of mass energy greatly exceeds the heavy quark masses, provides important tests of perturbative QCD. One particular area of theoretical interest [1–3] concerns the difference in charged particle multiplicity between heavy quark and light quark events. These differences are expected to arise from the suppression of gluon emission into the so-called ‘dead cone’ around the heavy quark direction.

In a previous publication [4] we used the apparent decay length of secondary vertices in a jet to select samples of events of different b purity and looked at the opposite side of the event to obtain values of the hemisphere charged particle multiplicity in $Z^0 \rightarrow b\bar{b}$ events, \bar{n}_b , compared to that in non $b\bar{b}$ events, \bar{n}_{uds} . Using the variation of c purity with decay length we also obtained the difference in charged particle multiplicity between b quark and light quark (u, d, s) events, $\delta_{bl} = 2 \times (\bar{n}_b - \bar{n}_{uds})$. Due to the small variation of c purity with decay length and its sensitivity to resolution effects, the systematic errors on \bar{n}_c were very large and a final result for the hemisphere charged particle multiplicity in $Z^0 \rightarrow c\bar{c}$ events, \bar{n}_c , was not given.

In this paper we present the first measurement of hemisphere charged particle multiplicity in $Z^0 \rightarrow c\bar{c}$ events. We use reconstructed D^* mesons to provide samples of events with varying c and b purity. By studying the charged particle multiplicity in the hemisphere opposite to the D^* in conjunction with samples of varying b purity from the decay length method, we are able to measure \bar{n}_{uds} , \bar{n}_c and \bar{n}_b separately. These measurements allow us to obtain the difference in charged particle multiplicity between c quark and light quark events, $\delta_{cl} = 2 \times (\bar{n}_c - \bar{n}_{uds})$ and to improve our measurement of δ_{bl} .

Combining our measurement of δ_{cl} with previous measurements at lower energies [5–7] allows the energy dependence of δ_{cl} to be compared to the predictions of models and QCD calculations for the first time.

2 Event Selection and Monte Carlo Simulation

A complete description of the OPAL detector can be found elsewhere [8]. Most of this analysis relies on the tracking of charged particles provided by the central detector, consisting of a silicon microvertex detector, a precision vertex drift chamber, a large volume jet chamber and chambers measuring the z -coordinate¹ of tracks as they leave the jet chamber.

The analysis is based on data recorded in 1991 after the silicon microvertex detector was commissioned, 1992 and 1993. Multihadronic Z^0 decays were selected using the criteria described in [9]. After data quality and detector performance requirements the data sample consisted of 1 707 683 events.

For the measurement of charged particle multiplicity, charged tracks were required to have at least 20 hits in the jet chamber, to have a measured momentum, p_t , in the x - y plane of at least

¹The OPAL coordinate system is defined with positive z along the electron beam direction and with positive x pointing roughly towards the centre of the LEP ring. The polar angle θ is defined relative to the $+z$ axis and the azimuthal angle ϕ relative to the $+x$ axis.

0.150 GeV/ c and to satisfy $|d_0| < 0.5$ cm, where d_0 is the distance of closest approach to the origin in the x - y plane. For the reconstruction of secondary vertices, tracks were additionally required to be associated with at least one hit in the silicon microvertex detector.

In each event, charged tracks and those electromagnetic clusters not associated to charged tracks, were grouped into jets using the jet cone algorithm described in [10] with cone half angle $R = 0.7$ rad and minimum jet energy $\epsilon = 7.0$ GeV. It was required that the two highest energy jets be in opposite hemispheres, where the hemispheres are defined with respect to the thrust axis calculated using the same tracks and clusters as used in the jet finding. In order that events be well contained in the detector, the cosine of the angle between the thrust axis and the beam axis was required to satisfy $|\cos \theta_{\text{thrust}}| < 0.8$. A total of 1 273 936 events satisfied these criteria.

Secondary vertices were reconstructed using the method described in [4]. To obtain event samples of varying b purity we used decay length significance (decay length divided by its error), as used in [11], rather than ordinary decay length, as used in [4], and the event by event beam position rather than the average beam position. With these changes the maximum attainable b purity was about 96%.

Simulated hadronic Z^0 decays were generated with the Jetset 7.3 [12] Monte Carlo program tuned to OPAL data as described in [13] using parameters described in [14] and using the Peterson fragmentation function [15] for c and b quarks. These events were passed through a detailed simulation [16] of the OPAL detector and subjected to the same pattern recognition and reconstruction algorithms as the data. These events were used to estimate the purity of the events with reconstructed vertices and to correct the charged particle multiplicity for detector effects.

3 D* Selection

The D^* mesons were reconstructed via the decay² $D^{*+} \rightarrow D^0 \pi^+ \rightarrow K^- \pi^+ \pi^+$. Charged tracks forming the D^* mesons were required to have at least 40 hits in the jet chamber, have $p_t > 0.250$ GeV/ c and to satisfy $|d_0| < 0.5$ cm.

The D^0 candidates were selected by taking all combinations of two oppositely charged tracks, with one of them assumed to be a pion and the other assumed to be a kaon. The D^* candidates were selected by combining D^0 candidates with a third track. This ‘slow pion’ track was required to have the same charge as the track presumed to be the pion in the D^0 decay. The D^* candidates were required to satisfy:

$$1.790 \text{ GeV}/c^2 < M_{D^0}^{\text{cand}} < 1.940 \text{ GeV}/c^2 \quad \text{and} \quad 0.142 \text{ GeV}/c^2 < \Delta M < 0.149 \text{ GeV}/c^2$$

where $\Delta M = M_{D^*}^{\text{cand}} - M_{D^0}^{\text{cand}}$ and $M_{D^*}^{\text{cand}}$ and $M_{D^0}^{\text{cand}}$ are the masses of the D^* and D^0 candidates respectively.

Making use of the fact that real D^0 mesons decay isotropically in their rest frames whereas the background is strongly peaked forwards and backwards, the following cuts were applied:

²Throughout this paper charge conjugate modes are always implied.

$|\cos\theta^*| < 0.8$ for $x_{D^*} < 0.5$ and $|\cos\theta^*| < 0.9$ for $x_{D^*} > 0.5$, where θ^* is the angle between the kaon in the D^0 rest frame and the direction of the D^0 in the laboratory frame and x_{D^*} is the scaled energy of the D^* , $x_{D^*} = 2E_{D^*}/E_{\text{cm}}$. For kaon candidate tracks with dE/dx information, the probability that the rate of energy loss, dE/dx , be consistent with that expected for a kaon was required to be greater than 10%. Finally, at least two of the three tracks were required to have either z -chamber hits or a z measurement derived from the point at which the track leaves the end of the jet chamber.

To provide samples with differing charm purity, the data were divided into three regions of x_{D^*} . Figure 1 shows the ΔM distribution in these three regions of x_{D^*} . The distributions have been fit with a Gaussian for the signal and with a functional form $A \exp(-B\Delta M)(\Delta M/m_\pi - 1)^C$ for the background [17]. These fits were used to determine the fraction of background, f_{BG} , in each D^* sample. The results of these fits are summarized in table 1.

	$0.2 < x_{D^*} < 0.4$	$0.4 < x_{D^*} < 0.6$	$0.6 < x_{D^*} < 1.0$
Number of D^* candidates	2240	932	526
Fraction of background f_{BG}	0.53	0.24	0.15
Estimated D^* signal	1052	707	449
c quark purity \mathcal{P}_c	0.22 ± 0.06	0.50 ± 0.06	0.90 ± 0.04
b quark purity \mathcal{P}_b	0.78 ± 0.06	0.50 ± 0.06	0.10 ± 0.04

Table 1: Summary of D^* signals and purity

In addition to the D^* sample, a wrong sign side-band sample was selected by requiring that the two pions of the D^* candidates had opposite charge and that $0.150 \text{ GeV}/c^2 < \Delta M < 0.170 \text{ GeV}/c^2$.

The c and b quark purities, \mathcal{P}_c and \mathcal{P}_b are defined as the fraction of D^* mesons originating in c quark and b quark events. These were obtained from the measured x distributions of D^* mesons in $Z^0 \rightarrow b\bar{b}$ and $Z^0 \rightarrow c\bar{c}$ decays given in [17]. In that analysis, the contributions from c quark events were separated from those from b quark events by a combination of bottom tagging methods using leptons, jet shape variables and lifetime information. Although the values given in [17] are corrected for detector efficiency and acceptance, no evidence was found that those corrections depended on whether the D^* was produced in a c or b event. In calculating the purities it was assumed that there is no contribution to D^* production from light quark events. Although D^* meson production from gluon splitting has been observed [17] at the few per cent level, consistent with theoretical expectations [18], it is concentrated mainly at low x_{D^*} . The Monte Carlo predicts that 0.3% of D^* mesons with $x_{D^*} > 0.2$ originate in light quark events. The c and b quark purities are given in table 1 for the three x_{D^*} bins.

At high x_{D^*} , D^* mesons are more likely to be found in high energy jets than low energy ones and therefore the hemispheres opposite are less likely to contain the highest energy jet. The hemisphere containing the highest energy jet (jet 1) also has a higher charged particle multiplicity on average than the hemisphere containing the second highest energy jet (jet 2) and so the sample of events containing D^* mesons with high x_{D^*} would have produced too low a value of \bar{n}_c . To overcome this bias, the whole analysis was performed separately for D^* mesons

in jet 1 and jet 2 and the (unweighted) average taken at the end.

4 Charged Particle Multiplicity

If a vertex fit was successful or a D^* was reconstructed in either of the two highest energy jets, the charged particle multiplicity in the hemisphere opposite that containing the jet was calculated. The hemispheres were defined by the thrust axis as described above. If vertices or D^* mesons were reconstructed in both hemispheres of an event then the multiplicity opposite each of them was used. If, however, a vertex and a D^* were reconstructed in the same hemisphere, then only the D^* information was used. Since there are many more vertices reconstructed than D^* mesons, this introduces negligible bias in the decay length sample.

The measured charged particle multiplicity was corrected for detector acceptance and efficiency as well as the introduction of spurious tracks from photon conversions and interactions using an unfolding matrix derived from the Monte Carlo simulation as described in [19]. No correction for initial state radiation was made. After this procedure, the multiplicity is defined as the total number of all promptly produced stable charged particles and those produced in the decays of particles with lifetimes shorter than 3×10^{-10} sec. This means that charged decay products from K_S^0 , hyperons and weakly decaying b and c flavoured hadrons are included in the definition, regardless of how far away from the interaction point the decay actually occurred.

The unfolding matrix was calculated separately for each bin of x_{D^*} or decay length significance. Applying the corrections increased the mean multiplicity, \bar{n} , by between 2% and 3%. Making no decay length or D^* cuts, a hemisphere multiplicity of 10.680 ± 0.004 was obtained, where the error is statistical only. This is to be compared with the published OPAL value of $10.70 \pm 0.02 \pm 0.19$ [19].

The corrected hemisphere multiplicities for each x_{D^*} bin were described by

$$\bar{n} = (1 - f_{BG})(\mathcal{P}_c \bar{n}_c + \mathcal{P}_b \bar{n}_b) + f_{BG} \bar{n}_{BG} \quad (1)$$

where the purities \mathcal{P}_c and \mathcal{P}_b were obtained from [17] as described above and the multiplicity opposite the D^* background, \bar{n}_{BG} , was obtained from the wrong sign side-band samples.

The corrected hemisphere multiplicities for each decay length significance bin were described by

$$\bar{n} = (1 - \mathcal{P}'_b) \bar{n}_{udsc} + \mathcal{P}'_b \bar{n}_b \quad (2)$$

$$\bar{n}_{udsc} = \frac{f_{uds} \bar{n}_{uds} + f_c \bar{n}_c}{f_{uds} + f_c} \quad (3)$$

where f_{uds} and f_c are the fractions of Z^0 events that decay to light quarks and $c\bar{c}$, respectively, in the Standard Model. In order to treat \bar{n}_{udsc} as a single variable in equation 2, small corrections of between -0.7% and 0.1% were applied to the decay length data to account for the varying charm contribution. These corrections were obtained from the Monte Carlo. The purity \mathcal{P}'_b as a function of decay length significance was obtained from the Monte Carlo as described in [4].

A simultaneous fit was performed on the D^* and decay length tagged data to extract \bar{n}_{uds} , \bar{n}_c and \bar{n}_b . In fact, the decay length data using equation 2 essentially fixes \bar{n}_{udsc} and \bar{n}_b and then

the D^* data provide \bar{n}_c through equation 1, allowing equation 3 to give \bar{n}_{uds} . The results of the fit were

$$\begin{aligned}\bar{n}_{uds} &= 10.41 \pm 0.06 \\ \bar{n}_c &= 10.76 \pm 0.20 \\ \bar{n}_b &= 11.81 \pm 0.01\end{aligned}$$

Weighting the results for \bar{n}_{uds} , \bar{n}_c , \bar{n}_b , according to the proportions of each flavour from the Standard Model, we obtain a hemisphere multiplicity of 10.78 ± 0.05 , where the error is statistical only. This is in good agreement with the OPAL published value given above.

Taking into account correlations between the results, the difference in charged particle multiplicity between c quark and b quark and light quark events is

$$\begin{aligned}\delta_{cl} &= 2 \times (\bar{n}_c - \bar{n}_{uds}) = 0.69 \pm 0.51 \\ \delta_{bl} &= 2 \times (\bar{n}_b - \bar{n}_{uds}) = 2.79 \pm 0.12\end{aligned}$$

5 Systematic Uncertainties

The systematic uncertainties affecting the decay length data are nearly the same as described in [4] except that the largest contribution due to uncertainties in the detector resolution has been reduced due to the higher b purity now obtained. The systematic uncertainties are summarized in table 2 and were estimated as follows:

- The cuts used to select D^* candidates were varied. The $M_{D^0}^{cand}$ window was increased to $1.765 \text{ GeV}/c^2 < M_{D^0}^{cand} < 1.965 \text{ GeV}/c^2$. The ΔM window was increased to $0.141 \text{ GeV}/c^2 < \Delta M < 0.150 \text{ GeV}/c^2$. Only one of the three tracks was required to have a z -chamber or jet chamber end point z measurement.
- The event purity of the D^* tagged sample, taken from [17], was varied within the errors quoted therein.
- The extent to which the wrong-sign sample correctly estimates the D^* background multiplicity is a possible source of systematic error. In order to estimate the effect on the final results we calculated the background multiplicity from side-bands with correct sign pions rather than the wrong signs and took the difference between these results and the standard results as an estimate of the systematic uncertainty. According to the Monte Carlo the difference between these two background estimates is slightly greater than the difference between the wrong sign estimate and the true background.
- As well as the bias towards high energy jets, the high x_{D^*} data produce a slight bias towards two jet events. The analysis was repeated for two jet and more than two jet events separately and the results averaged according to the ratio of two jets to more than two jets in the data. Alternatively we reweighted events so that the number of jets in events with D^* mesons was the same as in the whole data sample. The largest deviation from the standard result was used to estimate the systematic uncertainty due to this effect.

- The average b lifetime was varied by ± 0.10 ps about its central value of 1.55 ps [20].
- The Peterson parameters ϵ_b and ϵ_c , that control the b and c quark fragmentation, were varied from 0.0025 to 0.0080 and 0.026 to 0.066, respectively. These are equivalent to varying the mean scaled energies of the heavy quarks $\langle x_E \rangle_b$ and $\langle x_E \rangle_c$ in the ranges 0.70 ± 0.02 and 0.51 ± 0.02 , respectively, corresponding to the values given in [21, 17] but with slightly higher errors to allow for the fact that only one model has been considered here.
- The ratios $\Gamma_{b\bar{b}}/\Gamma_{\text{had}}$ and $\Gamma_{c\bar{c}}/\Gamma_{\text{had}}$ were varied in the ranges 0.217 ± 0.003 and 0.171 ± 0.045 respectively, corresponding to the value given in [11] and encompassing the value given in [17].
- The fractions of B_s and Λ_b produced in b quark fragmentation were changed from half to double their nominal values of 12% and 9% respectively, and the ratio of B_u to B_d was changed by $\pm 20\%$. The B hadron decay multiplicity (including K_S^0 and Λ decays) was varied by ± 0.5 tracks corresponding to the error given in [4].
- In the Monte Carlo, the difference between the x - y parameter d_0 of the reconstructed tracks and of their associated generated particles was increased by a factor of 1.4 to account for systematic misalignments in the data that were not included in the Monte Carlo simulation. This scaling factor was varied between 1.2 and 1.6 in order to estimate the uncertainty due to these effects.
- The analysis was repeated without correcting the decay length data for the variation of charm purity and for possible hemisphere to hemisphere correlations.
- Hemispheres tagged by decay length were not excluded if there was also a D^* tag.

Description	\bar{n}_{uds}	\bar{n}_c	\bar{n}_b	δ_{cl}	δ_{bl}
D^* selection cuts	0.021	0.079	0.001	0.199	0.043
D^* purity	0.020	0.068	0.000	0.174	0.038
D^* background multiplicity	0.018	0.059	0.003	0.156	0.043
Jet selection bias	0.011	0.004	0.005	0.023	0.033
b lifetime	0.008	0.001	0.003	0.016	0.018
b and c fragmentation	0.020	0.016	0.034	0.042	0.093
$\Gamma_{b\bar{b}}/\Gamma_{\text{had}}$ and $\Gamma_{c\bar{c}}/\Gamma_{\text{had}}$	0.040	0.016	0.034	0.104	0.116
B production and decay	0.007	0.012	0.056	0.018	0.120
d_0 resolution scaling	0.061	0.031	0.072	0.086	0.110
\bar{n}_{udsc} charm correction	0.002	0.049	0.066	0.097	0.132
Overlap exclusion	0.003	0.001	0.004	0.008	0.001
Total systematic error	0.085	0.136	0.123	0.353	0.270
Acceptance & efficiency	0.188	0.192	0.213	0.009	0.050

Table 2: Summary of systematic error contributions.

Since the same correction procedure as described in [19] has been used with essentially the same Monte Carlo program, it was assumed that this analysis is subject to the same acceptance and

efficiency systematic uncertainties as described in [19]. The contributions to the uncertainty in single hemisphere multiplicity are 0.2% from detector simulation, 1.5% from track and event selection and 0.9% from fragmentation model dependence giving an overall systematic uncertainty of 1.8%. This contribution should be treated as an overall scale uncertainty.

6 Comparison with Models and QCD Predictions

The results for \bar{n}_{uds} , \bar{n}_c and \bar{n}_b are shown in figure 2 along with the predictions of the Jetset 7.4 model with parameters tuned to OPAL data as described in [14]. The values predicted for \bar{n}_c and \bar{n}_b agree well with the data whereas the prediction for \bar{n}_{uds} is somewhat lower than the data.

The results for δ_{cl} and δ_{bl} are shown in figure 3 along with data from other experiments [5, 22, 6, 7, 23, 24] and the predictions of models and QCD calculations. The so-called naïve model [6] assumes that the non-leading multiplicity accompanying the heavy hadrons in heavy quark events is the same as the multiplicity in light quark events at the centre of mass energy corresponding to the energy left behind after the heavy quarks have fragmented. There are several variations of this model [2, 24] leading to slightly different predictions. We have used a form

$$\delta_{Ql} = 2N_Q^{\text{decay}} + \int \int N(\sqrt{(1-x_Q)(1-x_{\bar{Q}})W})f(x_Q)f(x_{\bar{Q}})dx_Qdx_{\bar{Q}} - N(W)$$

where $N(W) = 2.554 + 0.1252 \times \exp(2.317\sqrt{\ln W})$ is a parameterization of world average charged particle multiplicity data, corrected to remove the effects of heavy quark production [25], x_Q and $x_{\bar{Q}}$ are the fractions of the beam energy carried by the heavy hadrons, N_Q^{decay} is the decay multiplicity of the heavy hadrons, and W is the centre of mass energy. We approximated the fragmentation function $f(x_Q)$ by a normalized Peterson function with a mean of 0.51 ± 0.02 (0.70 ± 0.02) for charm (bottom) and used $N_Q^{\text{decay}} = 2.4$ (5.5). As seen from figure 3, the naïve model reproduces the data reasonably well at low energy but is somewhat below the data at high energy.

In QCD, the suppression of forward gluons in the angular region around the heavy quark direction leads to a lower multiplicity accompanying a heavy quark than a light quark at the same centre of mass energy. The total multiplicity is however higher in heavy quark events because of the additional particles from heavy hadron decay. Calculations [1] using MLLA [26] and LPHD [27] predicted that $\delta_{cl} = 1.7 \pm 0.5$ and $\delta_{bl} = 5.5 \pm 0.8$, independent of centre of mass energy. The previous measurements have already shown that the value of δ_{bl} is somewhat higher than the data but this is the first test of the prediction for δ_{cl} . Petrov and Kisselev [2] have modified these calculations to predict an absolute upper bound on δ_{cl} in the range 1.3 to 1.7, and on δ_{bl} in the range 3.7 to 4.1; the exact predicted values depending on the assumed heavy quark masses. They also calculate more representative values of $\delta_{cl} = 1.01$ and $\delta_{bl} = 3.68$ assuming $m_c = 1.5 \text{ GeV}/c^2$ and $m_b = 4.8 \text{ GeV}/c^2$. The prediction for δ_{cl} is in reasonable agreement with our data whereas δ_{bl} is still somewhat high.

The version of Jetset described above predicts $\delta_{cl} = 1.38$ ($\delta_{bl} = 4.15$) at $W=29 \text{ GeV}$ and $\delta_{cl} = 1.22$ ($\delta_{bl} = 3.27$) at $W=91 \text{ GeV}$.

7 Conclusions

We have used events with reconstructed D^* mesons to produce samples of events with varying charm purity. Combining these samples with those containing reconstructed secondary vertices which have high bottom purity, we have measured the hemisphere charged particle multiplicity in $Z^0 \rightarrow u\bar{u}, d\bar{d}, s\bar{s}$ events, $Z^0 \rightarrow c\bar{c}$ events and $Z^0 \rightarrow b\bar{b}$ events to be

$$\begin{aligned}\bar{n}_{uds} &= 10.41 \pm 0.06 \pm 0.09 \pm 0.19 \\ \bar{n}_c &= 10.76 \pm 0.20 \pm 0.14 \pm 0.19 \\ \bar{n}_b &= 11.81 \pm 0.01 \pm 0.12 \pm 0.21\end{aligned}$$

where the first error is statistical, the second systematic and the third is a common scale uncertainty. Taking into account correlations between the results, we find the difference in charged particle multiplicity between c quark events and light (u, d, s) quark events to be

$$\begin{aligned}\delta_{cl} &= 0.69 \pm 0.51 \pm 0.35 \\ \delta_{bl} &= 2.79 \pm 0.12 \pm 0.27.\end{aligned}$$

The values of \bar{n}_b and δ_{bl} supersede our previous results [4].

Acknowledgements

It is a pleasure to thank the SL Division for the efficient operation of the LEP accelerator and their continuing close cooperation with our experimental group. In addition to the support staff at our own institutions we are pleased to acknowledge the

Department of Energy, USA,

National Science Foundation, USA,

Particle Physics and Astronomy Research Council, UK,

Natural Sciences and Engineering Research Council, Canada,

Fussefeld Foundation,

Israel Ministry of Science,

Israel Science Foundation, administered by the Israel Academy of Science and Humanities,

Minerva Gesellschaft,

Japanese Ministry of Education, Science and Culture (the Monbusho) and a grant under the Monbusho International Science Research Program,

German Israeli Bi-national Science Foundation (GIF),

Direction des Sciences de la Matière du Commissariat à l'Énergie Atomique, France,

Bundesministerium für Forschung und Technologie, Germany,

National Research Council of Canada,

A.P. Sloan Foundation and Junta Nacional de Investigação Científica e Tecnológica, Portugal.

References

- [1] B.A.Schumm, Y.L.Dokshitzer, V.A.Khoze and D.S.Koetke, Phys. Rev. Letters **69** (1992) 3025.
- [2] V.A.Petrov and A.V.Kisselev, CERN-TH 7318/94.
- [3] J.Dias de Deus, Phys. Lett. **338B**(1994) 80.
- [4] OPAL Collaboration, R.Akers *et al.*, Z. Phys. C **61** (1994) 209.
- [5] TASSO Collaboration, M.Althoff *et al.*, Phys. Lett. **135B**(1984) 243.
The value of δ_{cl} was calculated using the value of \bar{n}_b given in [22] using the procedure described in [1].
- [6] Mark II Collaboration, P.C.Rowson *et al.*, Phys. Rev. Letters **54** (1985) 2580.
- [7] TPC Collaboration, H.Aihara *et al.*, Phys. Lett. **184B**(1987) 299.
- [8] OPAL Collaboration, K.Ahmet *et al.*, Nucl. Instr. and Meth. **A305** (1991) 275;
P.P.Allport *et al.*, Nucl. Instr. and Meth. **A324** (1993) 34;
P.P.Allport *et al.*, Nucl. Instr. and Meth. **A346** (1994) 476.
- [9] OPAL Collaboration, G.Alexander *et al.*, Z. Phys. C **52** (1991) 175.
- [10] OPAL Collaboration, R.Akers *et al.*, Z. Phys. C **63** (1994) 197.
- [11] OPAL Collaboration, R.Akers *et al.*, Z. Phys. C **65** (1995) 17.
- [12] T.Sjöstrand, Comp. Phys. Comm **39** (1986) 347;
T.Sjöstrand, M.Bengtsson, Comp. Phys. Comm **43** (1987) 367.
- [13] OPAL Collaboration, M.Z.Akrawy *et al.*, Z. Phys. C **47** (1990) 505.
- [14] OPAL Collaboration, P.D.Acton *et al.*, Z. Phys. C **58** (1993) 387.
- [15] C.Peterson, D.Schlatter, I.Schmitt and P.M.Zerwas, Phys. Rev. D **27** (1983) 105.
- [16] J.Allison *et al.*, Nucl. Instr. and Meth. **A317** (1992) 47.
- [17] OPAL Collaboration, R.Akers *et al.*, CERN-PPE/94-217, submitted to Z. Phys. C.
- [18] M.H.Seymour, Nucl. Phys. **B436** (1995) 163.
- [19] OPAL Collaboration, P.D.Acton *et al.*, Z. Phys. C **53** (1992) 539.
- [20] Particle Data Group, *Review of Particle Properties*, Phys. Rev. D **50** (1994) 1173.
- [21] OPAL Collaboration, R.Akers *et al.*, Z. Phys. C **60** (1993) 199.
- [22] TASSO Collaboration, W.Braunschweig *et al.*, Z. Phys. C **42** (1989) 17.

- [23] DELCO Collaboration, M.Sakuda *et al.*, Phys. Lett. **152B**(1985) 399;
 Mark II Collaboration, B.A.Schumm *et al.*, Phys. Rev. D **46** (1992) 453;
 TOPAZ Collaboration, K.Nagai *et al.*, Phys. Lett. **278B**(1992) 506;
 SLD Collaboration, K.Abe *et al.*, Phys. Rev. Letters **72** (1994) 3145.
 Some of the above experiments do not quote δ_{bl} directly but only \bar{n}_b and the total multiplicity. A summary of δ_{bl} values derived from these can be found in
 J.Chrin, *A study of the difference in charged multiplicity between bottom and light quark initiated events*, to appear in Proc. of the XXVII International Conference on High Energy Physics, Glasgow, UK, July 1994, IFIC-94-37-A (Sept 1994).
- [24] DELPHI Collaboration, P.Abreu *et al.*, CERN-PPE/95-01, submitted to Phys. Lett.
- [25] D.S.Koetke, *A measurement of the Z^0 hadronic branching ratio to bottom quarks and the charged multiplicity of bottom quark events using precision vertex detectors at $E_{cm} = 91$ GeV*, Ph.D Thesis SLAC-396.
- [26] Yu.L.Dokshitzer, V.A.Khoze, A.H.Mueller and S.I.Troyan, *Basics of Perturbative QCD*, ed. Tran Than Van, Editions Frontières, Paris, 1991.
- [27] D.Amati and G.Veneziano, Phys. Lett. **83B**(1979) 87;
 Ya.I.Azimov, Yu.L.Dokshitzer, V.A.Khoze and S.I.Troyan, Z. Phys. C **27** (1985) 65.

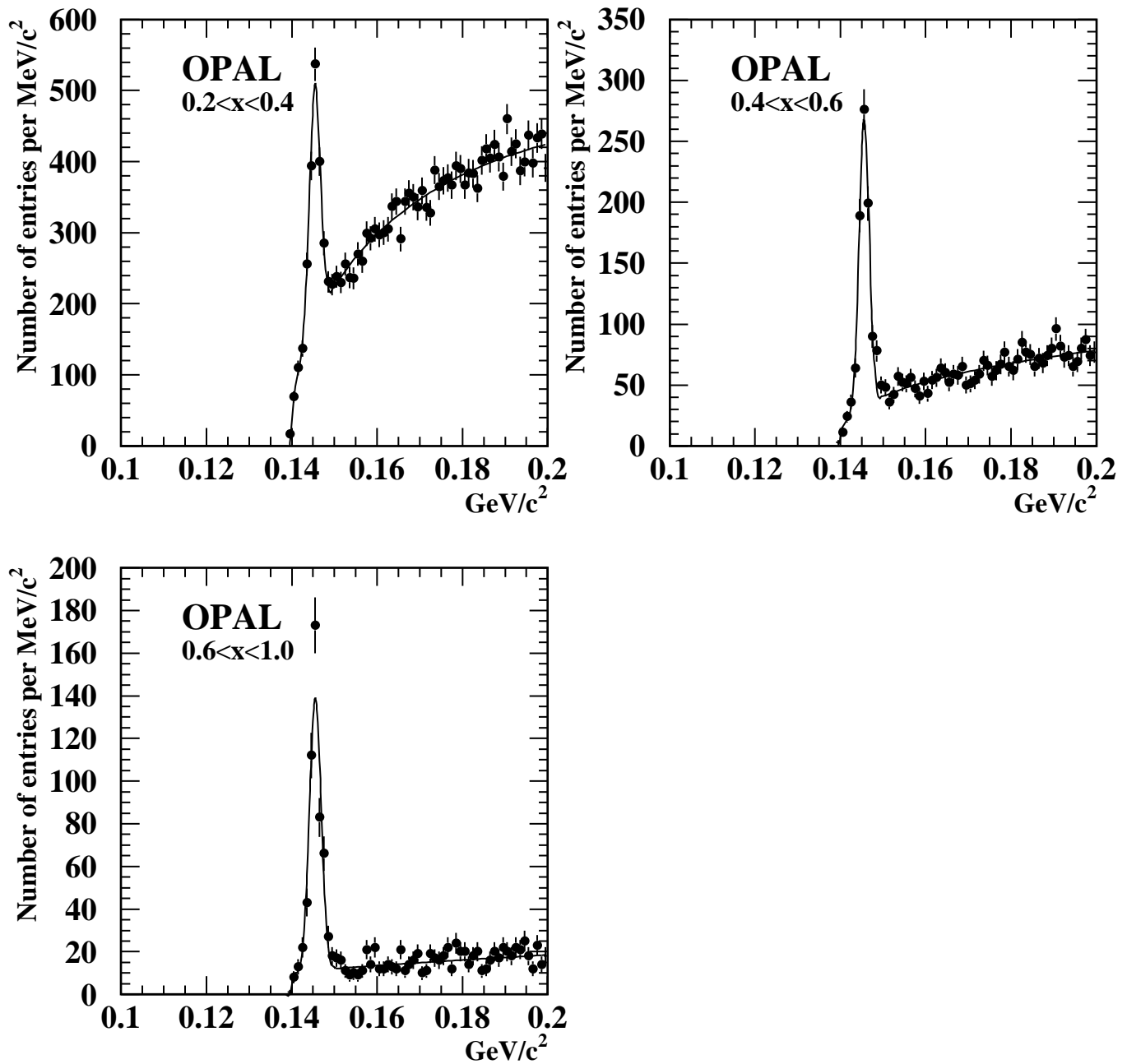


Figure 1: Distributions of the difference between the invariant mass of the D^* candidate and D^0 candidate in different x_{D^*} ranges. The points show the data while the solid lines are the results of the fits described in the text.

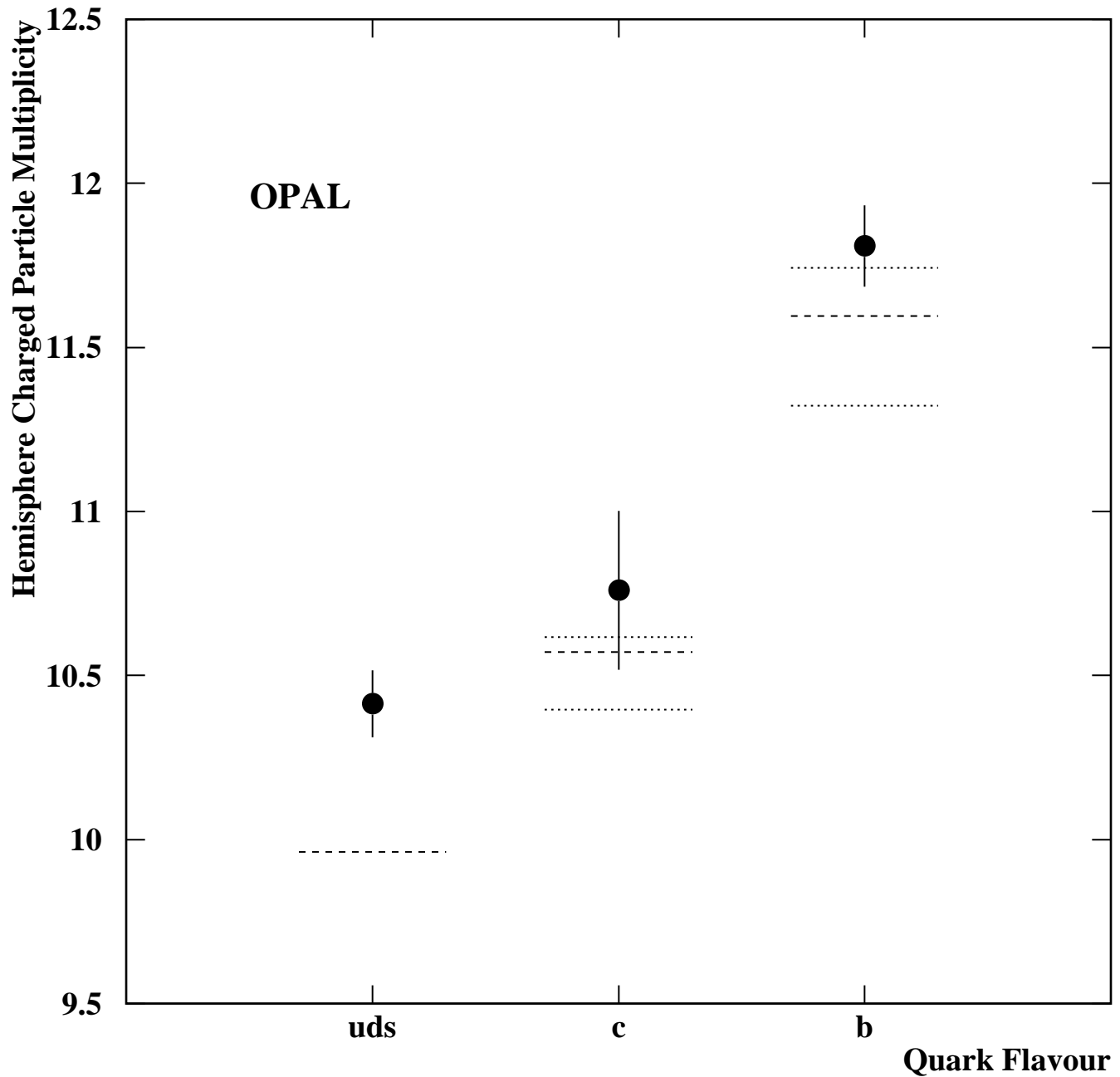


Figure 2: Values of the hemisphere charged particle multiplicities, \bar{n}_{uds} , \bar{n}_c and \bar{n}_b , obtained from the data. The error bars are the quadratic sum of the statistical and systematic errors but do not include the overall systematic scale uncertainty of 1.8%. The dashed horizontal lines are the predictions of Jetset 7.4 with the dotted lines reflecting the variation of the Peterson parameters ϵ_c and ϵ_b from 0.026 to 0.066 and 0.0025 to 0.0080 respectively; the multiplicity increases with ϵ .

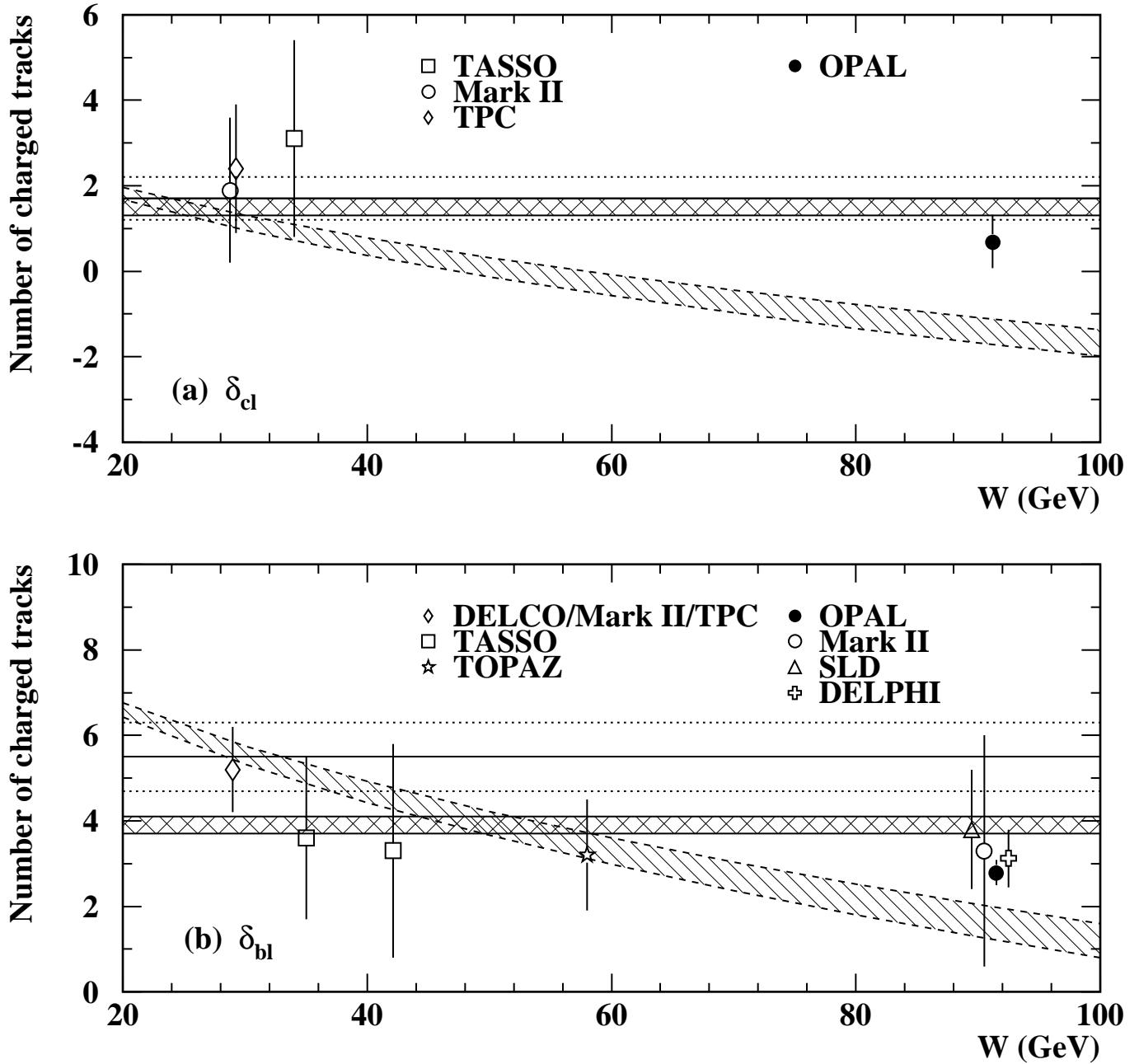


Figure 3: The difference in charged particle multiplicity between (a) c quark and light quark events, δ_{cl} and (b) b quark and light quark events, δ_{bl} , as a function of centre of mass energy. The single hatched areas represent the naive model while the cross hatched areas are the QCD upper limits as described in the text. The original MLLA predictions are shown as the solid lines with the dotted lines indicating the errors on these predictions not including higher order corrections. The data points around 91 GeV have been separated horizontally for clarity.